Stem Cell Research (2015) 15, 75–87

Available online at www.sciencedirect.com

ScienceDirect

www.elsevier.com/locate/scr

A chemically defined substrate for the expansion and neuronal differentiation of human pluripotent stem cell-derived neural progenitor cells

Yihuan Tsai, Josh Cutts, Azuma Kimura, Divya Varun, David A. Brafman*

School of Biological and Health Systems Engineering, Arizona State University, Tempe, AZ, 85287-9709, United States

Received 19 November 2014; received in revised form 4 May 2015; accepted 4 May 2015
Available online 13 May 2015

Abstract
Due to the limitation of current pharmacological therapeutic strategies, stem cell therapies have emerged as a viable option for treating many incurable neurological disorders. Specifically, human pluripotent stem cell (hPSC)-derived neural progenitor cells (hNPCs), a multipotent cell population that is capable of near indefinite expansion and subsequent differentiation into the various cell types that comprise the central nervous system (CNS), could provide an unlimited source of cells for such cell-based therapies. However the clinical application of these cells will require (i) defined, xeno-free conditions for their expansion and neuronal differentiation and (ii) scalable culture systems that enable their expansion and neuronal differentiation in numbers sufficient for regenerative medicine and drug screening purposes. Current extracellular matrix protein (ECMP)-based substrates for the culture of hNPCs are expensive, difficult to isolate, subject to batch-to-batch variations, and, therefore, unsuitable for clinical application of hNPCs. Using a high-throughput array-based screening approach, we identified a synthetic polymer, poly(4-vinyl phenol) (P4VP), that supported the long-term proliferation and self-renewal of hNPCs. The hNPCs cultured on P4VP maintained their characteristic morphology, expressed high levels of markers of multipotency, and retained their ability to differentiate into neurons. Such chemically defined substrates will eliminate critical roadblocks for the utilization of hNPCs for human neural regenerative repair, disease modeling, and drug discovery.

Introduction

Several neurodegenerative diseases and neural-related disorders are characterized by the damage to cells in the central nervous system (CNS). Human neural progenitor cells (hNPCs) derived from human pluripotent stem cells (hPSCs, including human embryonic stem cells [hESCs] and human induced pluripotent stem cells [hiPSCs]) can proliferate extensively and differentiate into all the neural lineages and supporting cells (i.e. neurons, astrocytes, and oligodendrocytes) that compromise the central nervous system (Chambers et al., 2009; Elkabetz et al., 2008; Shin et al., 2006). As such, there is great interest in the use of hNPCs for a variety of applications. First, hNPCs provide a unique opportunity to explore complex neural development processes in a simplified and accessible system. For example, hNPCs can provide an unlimited source of

* Corresponding author at: 501 E. Tyler Mall, ECG 334A, Tempe, AZ 85287, United States.
E-mail address: David.Brafman@asu.edu (D.A. Brafman).

http://dx.doi.org/10.1016/j.scr.2015.05.002
1873-5061/

neurons that can be used for a multitude of research studies ranging from cellular electrophysiology to protein biochemistry. Second, hNPCs and their derivatives generated from patients with genetic neural diseases can be used to provide important insights into disease pathology, progression, and mechanism (Marchetto et al., 2010; Imaizumi and Okano, 2013). Third, the ability to generate large quantities of human neural cells will enable the development of compounds and the screening of potential drugs for neurotoxicity (Betts, 2010; Bosnjak, 2012; Wilson et al., 2014). Lastly, because of the limited regenerative potential of the CNS, there is great promise for the use of hNPCs in cell replacement therapies (Yuan et al., 2011; Kakinohana et al.; Lu et al.; Hefferan et al., 2012). However, the use of hNPCs for such applications requires the development of efficacious and cost-effective defined culture systems for their large-scale expansion and differentiation.

The growth and differentiation of hNPCs depend on their microenvironment, including the chemical and physical properties of the extracellular matrix (ECM). However, current substrates used for hNPC expansion and differentiation, such as laminin (LN), are expensive, difficult to isolate, vary between lots, and contain xenogenic components which limit their use for clinical applications. Moreover, it has been reported that the heterogeneous composition of currently available matrices can lead to variable hNPC expansion rates, non-homogenous hNPC expansion, and inability of hNPCs to respond to differentiation signals (Bouhon et al., 2006; Li et al.). These limitations are a significant bottleneck in the clinical application of these cells where large quantities of homogenous hNPC and neuronal populations are required. In contrast, synthetic, polymer-based substrates that are inexpensive and easily fabricated represent a reliable alternative for the expansion and differentiation of hNPCs. Polymeric biomaterials have been utilized as substrates for the growth of a variety of adult stem cell types such as hematopoietic (Bagley et al., 1999; Banu et al., 2001; Berrios et al., 2001; Ehring et al., 2003) and mesenchymal stem cells (Curran et al., 2006; Kotobuki et al., 2008; Zhao et al., 2006; Fan et al., 2006; Richardson et al., 2008). More recently, we and others have developed polymeric materials that support the *in vitro* expansion of hPSCs in defined conditions (Villa-Diaz et al., 2010; Brafman et al., 2010; Mei et al., 2010; Zhang et al., 2013). However, polymeric materials as artificial matrices to support the growth and differentiation of hNPCs have not been developed.

In this study, we used a high-throughput screening approach to systematically screen a diverse library of synthetic polymers for their ability to support hNPC growth. Using this approach, we identified one polymer, poly(4-vinyl phenol) (P4VP), that supported the long-term growth and multipotency of hNPCs. In addition, P4VP was able to support the directed neuronal differentiation of hNPCs. This is the first example of long-term culture and neuronal differentiation of hNPCs on a chemically defined substrate free from exogenous extracellular matrix proteins (ECMPs).

Materials and methods

hNPC generation and culture

hNPCs were derived from HUES9, H9, HES3 and RiPSC (Warren et al., 2010) hPSCs as previously described (Brafman, 2014). Briefly, to initiate neural differentiation, hPSCs were cultured on Matrigel (BD Biosciences) in TeSR™2 defined medium (Stem Cell Technologies). Cells were then detached with treatment with Accutase (Millipore) for 5 min and resuspended in neural induction media [(1% N2/1% B27 without vitamin A/DMEM:F12), 50 ng/ml recombinant mouse Noggin (R&D Systems), 0.5 μM Dorsomorphin (Tocris Bioscience)] and 5 μM Y-27632 (Stemgent). Next, 7.5×10^5 cells were pipetted to each well of a 6-well ultra low attachment plates (Corning). The plates were then placed on an orbital shaker set at 95 rpm in a 37 °C/5% CO_2 tissue culture incubator. The next day, the cells formed spherical clusters (embryoid bodies [EBs]) and the media was changed to neural induction media. The media was subsequently changed every other day. After 5 days in suspension culture, the EBs were then transferred to a 10 cm dish coated (3 × 6 wells per 10 cm dish) with growth factor reduced Matrigel (1:25 in KnockOut DMEM; BD Biosciences) for attachment. The plated EBs were cultured in neural induction media for an additional 7 days. Neural rosettes were cut out by dissection under an EVOS (Life Technologies) microscope. Dissected rosettes were incubated in Accutase for 5 min and then triturated to single cells with a 1 ml pipet. Rosettes were then plated onto poly-L-ornithine (PLO; 10 μg/ml; Sigma) and mouse laminin (LN; 5 μg/ml; Sigma) coated dishes at a density of 12,500 cells/cm^2 in neural expansion media [(1% N2/1% B27 without vitamin A/DMEM:F12), 10 ng/ml mouse FGF2 (R&D Systems), and 10 ng/ml mouse EGF2 (R&D Systems)]. For routine maintenance, hNPCs were passaged onto PLO/LN-coated plates at a density of 10,000 cells/cm^2 in neural expansion media.

Polymer array fabrication

Arrays of polymers were fabricated as previously described (Brafman et al., 2010; Brafman et al., 2012). Briefly, glass slides were cleaned, silanized, and then functionalized with a polyacrylamide gel layer. Polymers were dissolved in the appropriate solvents (PBS, DMSO, DMF, or toluene) at a final concentration of 40 mg/ml. A list of polymers screened is provided in Supplementary Table 1. Polymers 1–10 were synthesized by free radical polymerization, polymers 11–80 were purchased from Sigma-Aldrich, and polymers 81–89 were purchased from PolySciences. A contact arrayer (SpotBot® 2, Arrayit®) was used to print the polymers. The printing conditions were a 1000 ms inking time and a 250 ms stamping time. Each spot had a diameter of 150–200 μm and neighboring spots were separated by a center-to-center distance of 450 μm. Slides were inspected manually under a light microscope for consistent and uniform polymer deposition. LN (250 μg/ml) was spotted as control and served as a reference to compare experiments from non-identical arrays. Prior to their use, array slides were soaked in PBS while being exposed to UVC germicidal radiation in a sterile flow hood for 10 min.

Culturing of hNPCs on polymer arrays

hNPCs were passaged (1.0×10^6 cells per slide) directly onto the slides and allowed to settle on the spots for 24 h prior to rinsing with neural expansion media 3 times to remove residual cells and debris. hNPCs were cultured on the arrays

for 7 days in neural expansion media. Culture media and growth factors were replenished daily.

Array slide staining, imaging, and quantification.

After 7 days of culture, the arrays were fixed for 15 min at room temperature (RT) with fresh paraformaldeyde (4% (w/v)). The arrays were washed twice with PBS and permeabilized with 0.2% (v/v) Triton-X-100 in PBS for 20 min at 4 °C. Cultures were then washed twice with PBS. Primary antibodies were incubated overnight at 4 °C and then washed twice with PBS at RT. Secondary antibodies were incubated at RT for 1 h. Antibodies used are listed in Supplementary Table S5. Nucleic acids were stained for DNA with Hoechst 33342 (2 μg/ml; Life Technologies) for 5 min at room temperature. Arrays were imaged using a CellInsight™ CX5 (Thermo Scientific) automated high-content screening platform. The system was programmed to visit each spot on the array, perform autofocus, and acquire Hoechst, FITC (SOX1), and Cy5 (NESTIN) images. Cell counts and stain intensities were measured using Thermo Scientific™ HCS Studio™ 2.0 Software using the built-in object identification and cell intensity algorithms.

hNPC expansion and neuronal differentiation on polymer-coated slides.

In order to coat the polyacrylamide-coated glass slides with the 'hit' polymers, 120 μl of each polymer (40 mg/ml) was placed dropwise into the center of the glass slide. A coverslip was placed on top of the glass slide to allow for uniform coating of the polymer. The polymer-coated slide was incubated for 1 h at 37 °C. The coverslip was then removed and the slide was washed 3 times with PBS prior to use. The presence of coated polymer was verified by FTIR-ATR (Supplementary Fig. 1). FTIR spectra were acquired on a Nicolet 6700 with Smart-iTR using a N_2 purged sample chamber. The acquisition parameters were: 128 scan and 4 cm^{-1} spectra resolution.

For hNPC expansion studies on polymer-coated slides, hNPCs were passaged (1.2×10^6 cells per slide) directly from PLO/LN plates onto the polymer-coated slides. hNPCs were maintained in neural expansion media. Culture media and growth factors were replenished daily. hNPCs were routinely passaged onto new polymer-coated slides every 5 days. For hNPC neuronal differentiation studies on polymer-coated slides, hNPCs were cultured in neuronal differentiation media [(0.5% N2/0.5% B27 without vitamin A/DMEM:F12), 20 ng/ml BDNF (R&D Systems), 20 ng/ml GDNF (R&D Systems), 1 μM DAPT (Tocris Bioscience), and 0.5 mM, dibutyrl-cAMP (db-cAMP; Sigma)] for 4 weeks.

Quantitative PCR (QPCR)

RNA was isolated from cells using the NucleoSpin® RNA Kit (Clontech). Reverse transcription was performed with qScript cDNA Supermix (Quanta Biosciences). Quantitative PCR was carried out using TaqMan® Assays or SYBR® green dye on a BioRad CFX96 Touch™ Real-Time PCR Detection System. For the QPCR experiments run with TaqMan® Assays a 10 min gradient to 95 °C followed by 40 cycles at 95 °C for 5 s and 60 °C for 30 s min was used. For QPCR experiments run with SYBR® green dye, a 2 min gradient to 95 °C followed by 40 cycles at 95 °C for 15 s and 60 °C for 1 min was used. The list of TaqMan® assays and primer sequences used is provided in Supplementary Table S4. Gene expression was normalized to 18S rRNA levels. Delta Ct values were calculated as $C_t^{target} - C_t^{18s}$. All experiments were performed with three technical replicates. Relative fold changes in gene expression were calculated using the $2^{-\Delta\Delta Ct}$ method (VanGuilder et al., 2008). Data are presented as the average of the biological replicates ± standard error of the mean (SEM).

Immunofluorescence

Cultures were gently washed twice with staining buffer (PBS w/1% (w/v) BSA) prior to fixation. Cultures were then fixed for 15 min at room temperature (RT) with fresh paraformaldeyde (4% (w/v)). The cultures were washed twice with staining buffer and permeabilized with 0.2% (v/v) Triton-X-100 in stain buffer for 20 min at 4 °C. Cultures were then washed twice with staining buffer. Primary antibodies were incubated overnight at 4 °C and then washed twice with stain buffer at RT. Secondary antibodies were incubated at RT for 1 h. Antibodies used are listed in Supplementary Table S5. Nucleic acids were stained for DNA with Hoechst 33342 (2 μg/ml; Life Technologies) for 5 min at room temperature. Imaging was performed using an automated confocal microscope (Olympus Fluoview 1000 with motorized stage). Quantification of images was performed by counting a minimum of 9 fields at 20× magnification. Image quantification of the data is presented as the average of these fields ± standard deviation (SD). Cell length and cell area measurements were conducted on 45 cells from 3 fields at 20× magnification at each time point using Image J.

Population doubling time

Population doubling time of hNPCs cultured on LN and P4VP substrates was calculated using the following equation: PDT (*h*) = (T2 − T1) / (3.32 * [log(N2) − log(N1)]).

Flow cytometry

Cells were dissociated with Accutase for 5 min at 37 °C, triturated, and passed through a 40 μm cell strainer. Cells were then washed twice with FACS buffer (PBS, 10 mM EDTA, and 2% FBS) and resuspended at a maximum concentration of 5×10^6 cells per 100 μl. One test volume of antibody was added for each 100 μl cell suspension (Supplementary Table S5). Cells were stained for 30 min on ice, washed, and resuspended in stain buffer. Cells were analyzed and sorted with a FACSCanto (BD Biosciences). Flow cytometry data was analyzed with FACSDiva software (BD Biosciences). Isotype negative controls are listed in Supplementary Table S5.

Results

Polymer microarray screen with hNPCs

We have previously described the development of a high-throughput microarray technology for the systematic

investigation of the effects of polymeric biomaterials on stem cell fate (Brafman et al., 2010). Briefly, we used a contact DNA microarray spotting instrument to deposit nanoliter amounts of polymer solutions onto glass microscope slides coated with a layer of acrylamide gel (~10 μm thick). The spotted polymer chains are mechanically interlocked with the underlying acrylamide gel and anchored in place after solvent evaporation. Each polymer spot is 150–200 μm in diameter with a center-to-center distance of 450 μm. Cells are globally seeded onto the arrays and due to the non-fouling nature of the acrylamide hydrogel cells only adhere to sites of polymer deposition. As we have previously shown (Brafman et al., 2010; Brafman et al., 2012; Brafman et al., 2009a; Brafman et al., 2013; Brafman et al., 2009b), paracrine signaling between neighboring spots is limited and each spot can be treated an independent 'well'. Combined with high-content automated microscopy which allows for quantitative single-cell analysis, this technology can be used to screen the effect of thousands of unique polymer compositions on the fate of any cell type of interest on a single microscope slide.

We utilized this array technology to identify polymers that support hNPC adhesion, growth, and multipotency (Fig. 1A). hNPCs were derived from hPSCs and expanded on laminin (LN)-coated substrates in the presence of bFGF and EGF as previously described (Brafman, 2014). Prior to seeding onto the array, expanded hNPCs were routinely assessed for their characteristic morphology and maintenance of markers of hNPC multipotency such as SOX1 and NESTIN (Fig. 1A). Biomaterials often mediate cell adhesion through integrin-mediated interactions between the cells and extracellular matrix proteins (ECMPs) that have been absorbed from the surrounding media (Shin et al., 2003). To eliminate the undefined absorption of these soluble ECMPs, we performed all of our screens in the presence of a medium (see Materials and methods) which contained no soluble ECMPs. As such, any observed interaction between a specific polymer and hNPCs would be independent of exogenously absorbed soluble ECMPs.

To seed the polymer arrays, hNPCs were enzymatically dissociated into single cells, and cell suspensions were

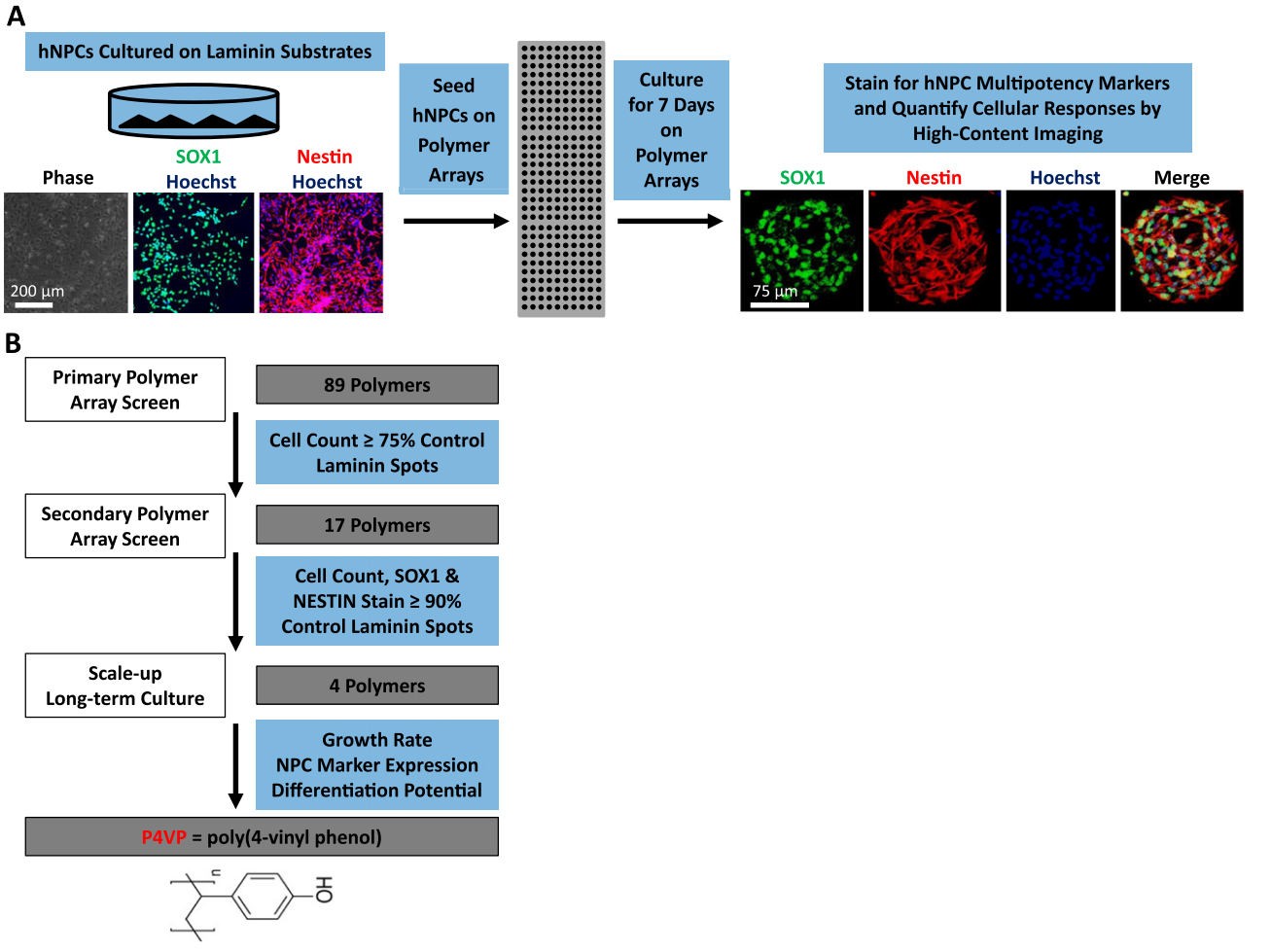

Figure 1 High-throughput screening of polymers for hNPC growth. (A) Schematic representation of polymer array assay. Prior to seeding onto the array, hNPCs were cultured on PLO/LN substrates and routinely assessed for their characteristic morphology and maintenance of hNPC multipotency markers SOX1 and NESTIN. hNPCs were cultured on the polymer arrays for 7 days and imaged by automated high-content microscopy. hNPCs were assessed for their proliferation (Hoechst) and maintenance of a multipotent hNPC phenotype (SOX1 and NESTIN). (B) Screening paradigm used for identification of polymers that support hNPC attachment, growth, and maintenance of multipotency.

allowed to settle onto the polymer spots for 24 h. Subsequently, the medium was replaced to remove non-adhering cells and debris. Seeding the slide with 1.0×10^6 hNPCs allowed for the attachment of 5–10 cells per spot and provided sufficient area for growth. hNPCs were allowed to grow for 7 days in the presence of FGF2 and EGF, which maintain hNPCs in a proliferative, multipotent state. After 7 days, the cells were stained for the hNPC multipotency markers SOX1 and NESTIN and high-content imaging was used to count cells and measure SOX1 and NESTIN intensities at a single-cell level (Fig. 1A).

Using the polymer array technology, we screened a library of diverse polymers with varying functional groups, charge density, hydrophobicity, and molecular weight (Supplemental Table 1). For instance, since heparin modulates the activity of bFGF and EGF (Burgess and Maciag, 1989; Bellosta et al., 2001), growth factors that play crucial roles in self-renewal of NPCs, this library contains several heparin-mimicking polymers with sulfate and carboxyl functional groups. Our approach consisted of two rounds of screening, resulting in the identification of several 'hits', which we subsequently scaled-up and assessed for their ability to support long-term hNPC expansion (Fig. 1B). In the first round of screening, each polymer was tested individually at a single concentration (40 mg/ml). As a control we used LN, which supports the adhesion and growth of hNPCs. After 7 days, cells were stained with a DNA stain (Hoechst) and the number of cells per spot was counted by automated high-content imaging (Fig. 2A and Supplemental Table 2). For the first round of screening, a 'hit' was defined as a polymer supporting the average cell number (across 5 replicate spots) $\geq$75% of the average cell number on the control LN spots. By this criterion, we identified 17 polymer 'hits' in our first round of screening (Fig. 2B). In the second round of screening, these top 'hits' were rescreened and assessed for their ability to support the short-term growth (determined by cell number) and multipotency (determined by SOX1 and NESTIN expression) of hNPCs (Fig. 2C and Supplemental Table 3). For the second round of screening, a 'hit' was defined as a polymer supporting the average cell number and SOX1/NESTIN expression (across 8 replicate spots) $\geq$90% of hNPCs grown on control LN spots (Fig. 2D). From this second screen, 4 polymers demonstrated the ability to support growth and maintenance of multipotency at similar levels as LN (Fig. 2E).

Long-term culture of hNPCs on defined polymer substrate

In order to investigate the scalability of the 4 'hit' polymers physicochemical properties and ability to support long-term hNPC growth, acrylamide gel-coated slides were coated with the 'hit' polymers by thermal evaporation (see Materials and methods). The presence of polymer coating was verified by FTIR-ATR (Supplemental Fig. 1). hNPCs were enzymatically detached from LN-coated substrates and passaged onto the polymer-coated slides. Detachment or spontaneous differentiation, as indicated by changes in morphology was observed on all the 'hit' polymers with the exception of poly(4-vinyl phenol) (P4VP; Fig. 3A and B).

Next, we tested the ability of P4VP to support hNPC expansion over 10 passages (~50 days). hNPCs cultured on P4VP substrates maintained their characteristic morphology over the 10 passages (Fig. 4A). Additionally, hNPCs cultured on PV4P exhibited similar growth dynamics (Fig. 4B) and doubling time (Fig. 4C) to cells cultured on LN substrates. Moreover, the rate of cell growth on P4VP substrates remained stable during the 10 passages (Fig. 4D). In fact, cell counts taken at each passage revealed that 1×10^6 hNPCs could theoretically be expanded to 1×10^9 hNPCs over 10 passages (Fig. 4D). Maintenance of a hNPC phenotype was assessed by quantitative RT-PCR for hNPC makers *SOX1*, *SOX2*, and *NESTIN* (Fig. 4E). hNPCs grown on P4VP maintained expression of these markers at levels similar to that of cells grown on LN substrates. Along similar lines, flow cytometry (Fig. 4F) and immunostaining (Fig. 4G) revealed that hNPCs cultured on P4VP-coated substrates for 10 passages continued to express high levels of the hNPC markers SOX1, SOX2, and NESTIN. Together, these results demonstrate the ability of P4VP to support the long-term culture of hNPCs.

Because P4VP could support the long-term growth of hNPCs, we wanted determine if P4VP could be used as a matrix for the derivation of hNPCs. To that end, we plated EBs directly onto LN- and P4VP-coated substrates. In comparison to EBs plated onto Matrigel-coated plates, EBs plated directly onto LN or P4VP matrices failed to form neuroepithelial-like rosettes (Supplemental Fig. 2A). Similarly, while dissected rosettes plated onto LN substrates resulted in the formation of hNPCs, rosettes replated on P4VP-coated surfaces did not result in the generation of hNPCs. However, dissociated rosettes initially replated onto LN substrates and then subsequently transferred to P4VP substrates resulted in the formation of cells representative of hNPCs (Supplemental Fig. 2B). In fact, hNPCs continually cultured on PLO/LN or transitioned to P4VP substrates displayed similar morphology (Supplemental Fig. 2B), growth rate (Supplemental Fig. 2C and D), and expression of hNPC markers SOX2 and NESTIN (Supplemental Fig. 2E).

Neuronal differentiation of hNPCs on defined polymer substrate

Because of the dynamic nature of cell–substrate interactions during stem cell differentiation (Brafman et al., 2013; Marthiens et al., 2010; Dalby et al., 2014; Wojcik-Stanaszek et al., 2011), the same synthetic substrate may not be suitable for both hNPC expansion and neuronal differentiation. To that end, we assessed the ability of P4VP to support the directed neuronal differentiation of hNPCs. Specifically, hNPCs were seeded onto P4VP substrates and differentiated to neurons through the withdrawal of bFGF and EGF, and addition of neuronal inducing factors brain-BDNF, GDNF, db-cAMP, and the Notch inhibitor DAPT. After 4 weeks in the presence of neuronal induction factors, cells cultured on P4VP substrates acquired a neuronal morphology (Fig. 5A). Immunofluorescence revealed that a high percentage of the cells stained positive for the pan-neuronal markers NeuN (Fig. 5B), neurofilament-68 (NF-L; Fig. 5C), microtubule-associated protein 2 (MAP2; Fig. 5D) and β-Tubulin-III (β3T;

Fig. 5E). In fact, quantitative RT-PCR revealed that cells differentiated on P4VP expressed higher levels of MAP2 and β3T than those differentiated on LN substrates (Fig. 5F). Along similar lines, neuronal differentiation of NPCs on P4VP resulted in a higher number of MAP2 and β3T positive neurons than NPCs differentiated on LN substrates (Fig. 5G). Collectively, this data indicates that in addition to supporting the long-term expansion of hNPCs that P4VP can also serve as an effective neuronal differentiation matrix.

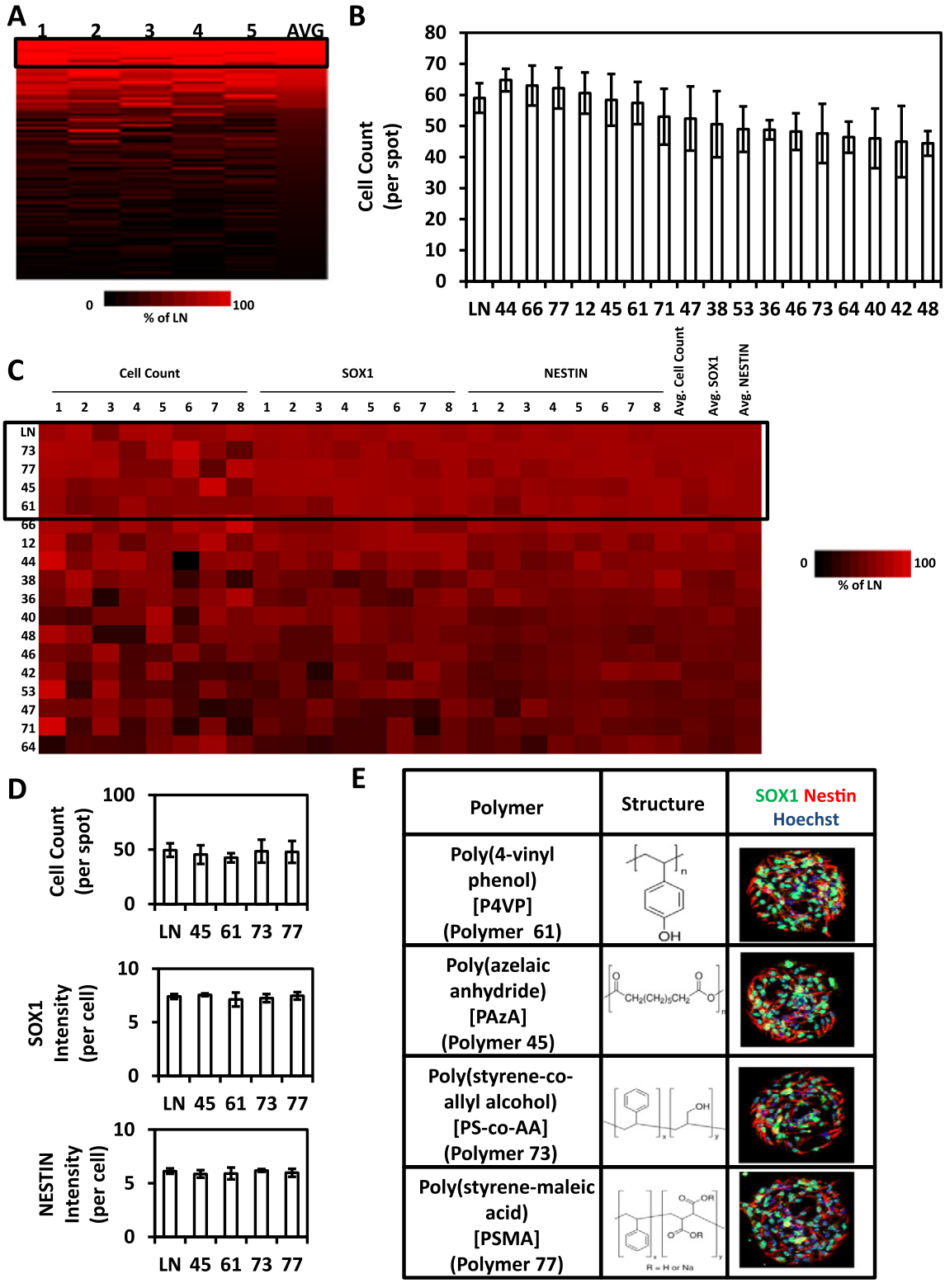

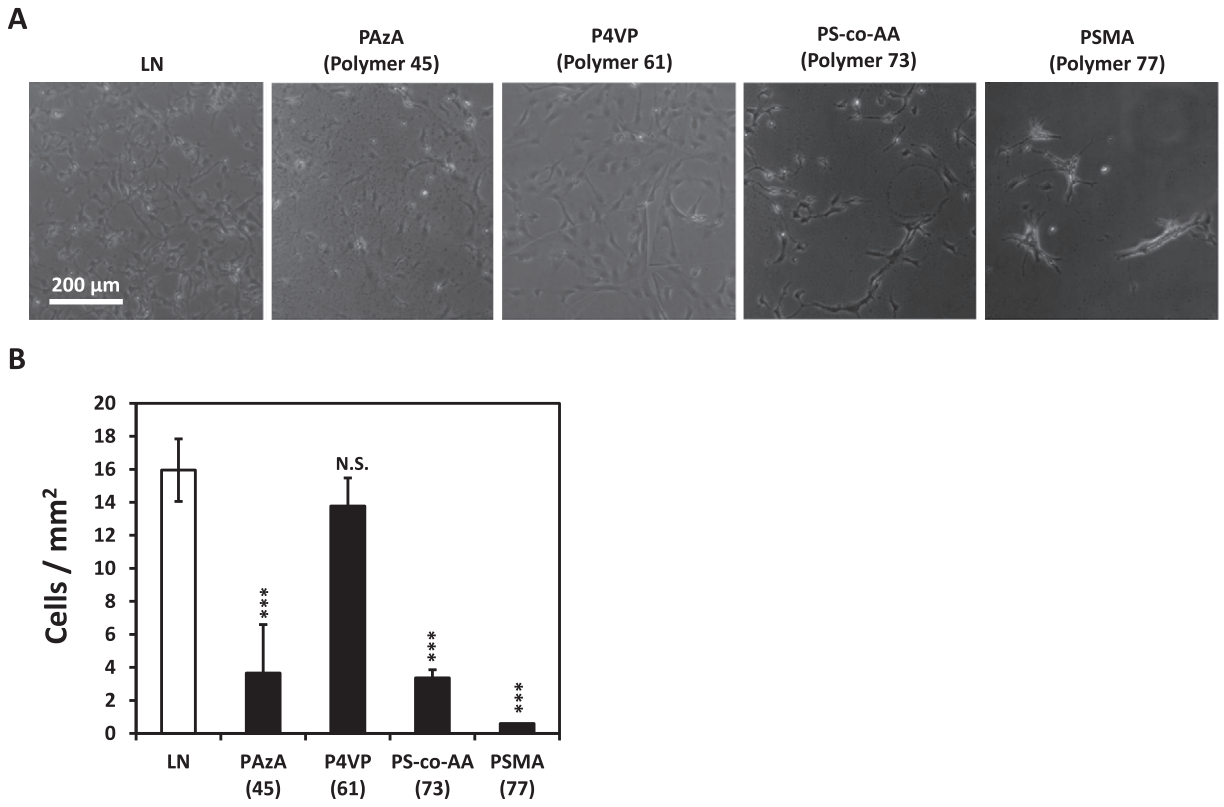

Figure 3 Scalability of 'hits' identified from polymer array screen. (A) Phase contrast images of hNPCs cultured on glass slides coated with laminin (LN) and the 4 'hit' polymers: poly(4-vinyl phenol) [P4VP], poly(azelaic anhydride) [PAzA], poly(styrene-co-allyl alcohol) [PS-co-AA], and poly(styrene-maleic acid) [PSMA]. (B) Cell count of hNPCs cultured on the 'hit' polymer- and LN-coated slides for 5 days. Quantification of images was performed by counting a minimum of 9 fields at 20× magnification. Image quantification of the data is presented as the average of these fields ± standard deviation (SD). Cell counts on polymers were compared to cell counts on LN controls using Student's *t*-test. ***$p < 0.001$, N.S. = not statistically significant.

Mechanism of hNPC attachment and growth on P4VP substrates

To elucidate the mechanism of hNPC attachment and growth on P4VP substrates, we performed time-lapse imaging of initial hNPC attachment on P4VP and LN-coated substrates (Fig. 6A). Quantitative analysis of the dynamics of cell length (Fig. 6B) and cell area (Fig. 6C) revealed that initial hNPC attachment and spreading significantly differed on P4VP and LN substrates. While hNPCs immediately adhered and spread on LN substrates, cells on P4VP remained rounded for several hours prior to achieving a similar level of adhesion and spreading as hNPCs cultured on LN substrates.

To determine if these differences in cell spreading rates could be explained by differences in endogenous ECMP expression, we analyzed the kinetics of the expression levels of genes encoding several ECMPs that have previously been shown to influence hNPC fate (Li et al., 2012; Ma et al., 2008; Gil et al., 2009; Li et al., 2014) including collagen I (*COL1*), collagen IV (*COL4*), fibronectin (*FN*), laminin (*LN*), and vitronectin (*VTN*) (Fig. 6D). The expression levels of endogenous ECMPs of hNPCs cultured on LN substrates peaked upon initial adhesion (1 h) but quickly decreased upon subsequent culture. On the other hand, hNPCs cultured on P4VP showed prolonged expression of endogenous ECMPs with expression decreasing only after 12 h of culture. This

Figure 2 Analysis of hNPCs on polymer arrays. (A) Heat map for the first round of polymer array screening in which the cell number for each polymer (row) on each replicate spot (column) has been quantified. Values were normalized to the average number of cells on the control LN spots. The rows are arranged from high to low based on the average value among replicate spots ($n = 5$). A black box denotes the polymers with an average cell number $\geq 75\%$ of the average cell number on the control LN spots. (B) The average cell number on the 17 'hit' polymers and LN control spots (mean ± SEM, $n = 8$). (C) Heat map for the second round of polymer array screening in which the number and SOX1/NESTIN expression of cells on each polymer (row) on each replicate spot (column) has been quantified. Values were normalized to the average values of cells on the control LN spots. The rows are arranged from high to low based on the average value of all three parameters among replicate spots ($n = 8$). A black box denotes the polymers with an average cell number and NESTIN/SOX1 expression $\geq 90\%$ of hNPCs grown on control LN spots. (D) The average cell number and NESTIN/SOX1 intensities of hNPCs on the 4 'hit' polymers and LN control spots (mean ± SEM, $n = 8$). (E) Chemical structures of 'hit' polymers and representative immunofluorescent images of hNPCs on 'hit' polymer spots.

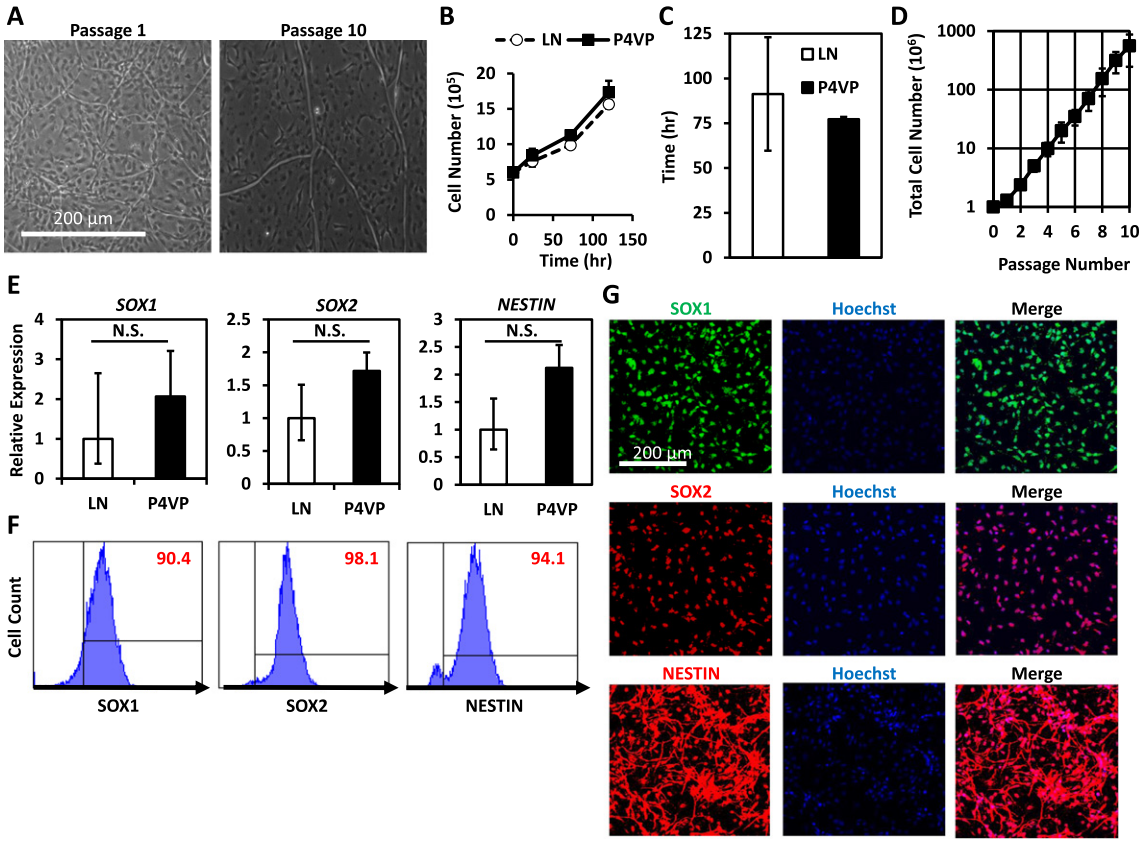

Figure 4 Long-term expansion of hNPCs on P4VP. (A) Phase contrast images of hNPCs cultured on P4VP for 10 passages. (B) Growth rate of hNPCs on P4VP and LN (mean ± SEM, $n = 3$). (C) Doubling time of hNPCs cultured on P4VP and LN (mean ± SEM, $n = 3$). (D) hNPCs were cultured on P4VP for 10 passages and cell growth was analyzed by cell count at each passage (mean ± SEM, $n = 3$). (E) Gene expression analysis of *SOX1*, *SOX2*, and *NESTIN* of hNPCs cultured on P4VP and LN for 10 passages (mean ± SEM, $n = 3$). Populations were compared using Student's *t*-test. N.S. = not statistically significant. (F) Flow cytometry and (G) immunofluorescent analysis of hNPCs cultured on P4VP for 10 passages. Isotype controls used are listed in Supplementary Table 5.

time point coincided with the time point at which cells cultured on P4VP showed a similar level of spreading as hNPCs cultured on LN substrates.

We also measured the expression levels of the integrin cell surface proteins known to mediate cell adhesion to these ECMPs (Humphries et al., 2006) (Fig. 6E). Similar to the dynamics of the endogenous ECMP expression, the expression levels of α-integrins 1–3, 5 and v, and β integrins 1, 3, and 5 of hNPCs cultured on LN peaked upon initial adhesion (1 h) but rapidly declined upon subsequent culture. In contrast, peak expression of these integrins in hNPCs cultured on P4VP substrates was delayed and did not significantly decrease until after 12 h in culture. Together, these differences in cell spreading and attachment as well as endogenous ECMP and integrin expression dynamics suggest a possible mechanism by which initial hNPC attachment on P4VP is supported through an integrin-ECMP independent interaction. In turn, this temporary interaction allows the cells to secrete their own ECMPs and assemble a microenvironment to support further spreading and adhesion.

Discussion

The use of hNPCs for disease modeling, drug screening, or cell therapies requires the development of efficacious and cost-effective defined substrates for their expansion and neuronal differentiation. In this study, we employed an unbiased, high-throughput screening approach to systematically screen a diverse library of chemically defined polymers for the *in vitro* expansion and neuronal differentiation of hNPCs. Although most of the polymers screened were unable to support the long-term expansion of hNPCs, we identified one polymer, P4VP, which was able to support the long-term culture of hNPCs over multiple passages. In fact, hNPCs cultured on these synthetic substrates maintained their characteristic morphology while growing at a similar rate and expressing similar levels of multipotent NPC markers as cells cultured on LN substrates. Additionally, in the presence of neuronal inducing factors, hNPCs efficiently differentiated to cells representative of neurons.

The mechanism by which P4VP supports hNPC expansion is not entirely clear. Live cell imaging revealed that hNPCs cultured on P4VP had delayed cell attachment and spreading kinetics. Additionally, we found that hNPCs cultured on P4VP showed increased and prolonged expression of several endogenous ECMPs and the integrins known to mediate cell attachment to these specific ECMPs. Because the media used for hNPC culture was free of exogenous ECMPs, we speculate that P4VP fosters initial hNPC adhesion in an ECMP-independent manner, possibly through electrostatic

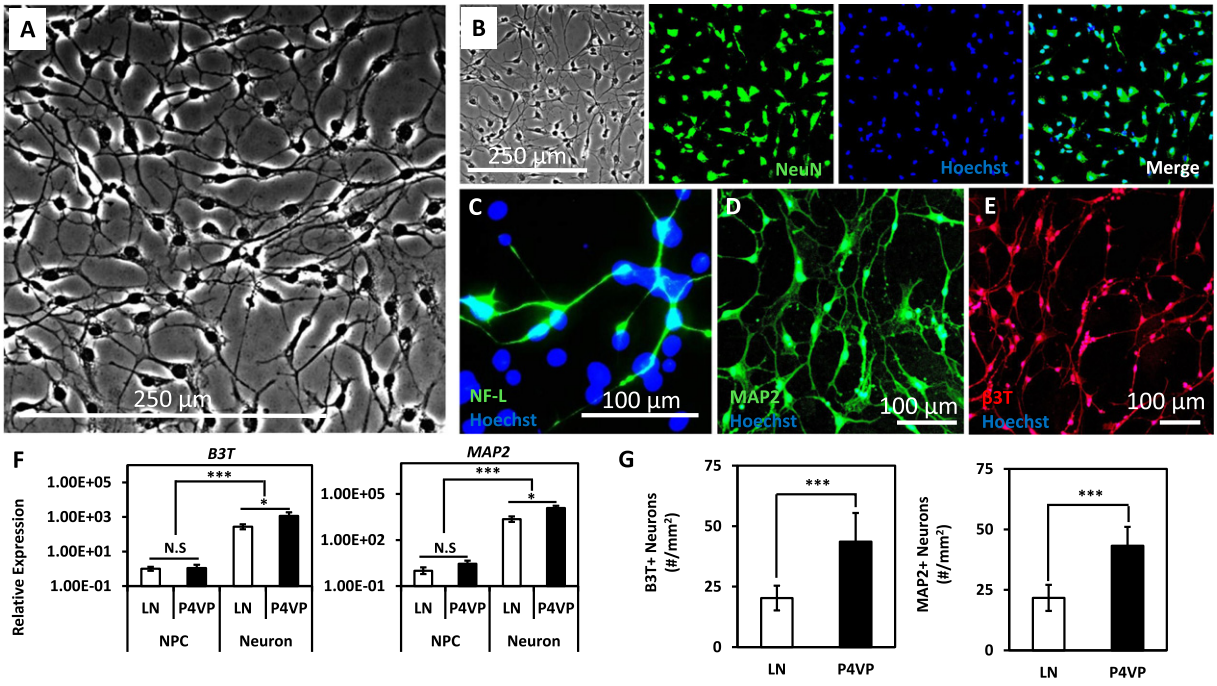

Figure 5 Neuronal differentiation of hNPCs on P4VP. (A) Phase contrast images of neurons differentiated on P4VP. (B) Phase contrast and immunofluorescence of mature neuronal markers NeuN, (C) NF-L, (D) MAP2 and (E) B3T in neuronal cultures differentiated on P4VP. (F) Gene expression analysis of *MAP2* and *B3T* of neuronal cultures differentiated on P4VP and LN substrates (mean ± SEM, $n = 3$). Populations were compared using Student's t-test. * $p < 0.05$, ** $p < 0.01$. (G) Quantification of the number of MAP2- and B3T-positive neurons generated on P4VP and LN substrates. Quantification of images was performed by counting a minimum of 9 fields at 20× magnification. Image quantification of the data is presented as the average of these fields ± standard deviation (SD). Populations were compared using Student's t-test. *** $p < 0.001$.

interactions between the cells and the substrate (Smetana et al., 1992; Kirby et al., 2003; Lampin et al., 1997; Lofti et al., 2013). Subsequently, the cells secrete their own ECMPs, which delays attachment and spreading, but ultimately provides a suitable microenvironment for cell attachment and continued growth.

Although P4VP could support the expansion and differentiation of hNPCs, it did not serve as a robust substrate for the derivation of hNPCs. Specifically, unlike EBs plated onto Matrigel-coated plates which spread out and formed neuroepithelial-like rosettes, EBs plated directly onto P4VP- or LN-coated substrates failed to form rosette-like structures. Along similar lines, while dissected rosettes generated on Matrigel-coated plates led to the formation of hNPCs upon replating on LN substrates, rosettes plated on P4VP-coated surfaces did not result in the generation of cells representative of hNPCs. However, dissociated rosettes that were initially replated onto LN substrates and then subsequently transferred to P4VP substrates led to the generation of cells representative of hNPCs. This suggests that hNPCs may require a brief transition period in which dissected rosettes need to be initially cultured on LN substrates after which cells can be transitioned to P4VP substrates. In the future, polymer array screens can be performed to identify such synthetic substrates that directly support the derivation of hNPCs.

Interestingly, we found that neuronal differentiation of hNPCs was significantly enhanced on P4VP compared to cells differentiated on LN-coated culture surfaces. During *in vivo* neural development, the ECM undergoes dynamic changes in response to soluble signaling molecules to regulate cell proliferation, migration, and differentiation (Pavlov et al., 2004; Barros et al., 2010; Wade et al., 2014). Along similar lines, several *in vitro* studies have shown that ESC-derived NPCs have specific substrate requirements to promote self-renewal versus those needed to instruct neuronal specification (Ma et al., 2008; Goetz et al., 2006). As such, ECMPs, such as LN, have distinct and temporally specific effects during ESC-derived NPC expansion and neuronal differentiation (Ma et al., 2008; Goetz et al., 2006). Because cell–substrate interactions change as stem cells shift from a state of self-renewal to one of differentiation, we speculate that P4VP provides a more permissive environment in which hNPCs can respond to the exogenous soluble signaling microenvironment and synthesize the necessary ECMP environment needed for self-renewal or neuronal differentiation.

Arrays of polymers have been used by several groups as a high-throughput means to develop polymer-based matrices that support the self-renewal, proliferation, and differentiation of a variety of stem cell types (Brafman et al., 2010; Anderson et al., 2004; Hansen et al., 2014). Moreover, such technologies have been successfully used to identify specific biomaterial properties that precisely direct stem cell fate (Mei et al., 2010). In one such study, it was demonstrated that specific chemical functional groups could be used to direct the differentiation of human mesenchymal stem cells into either osteoblasts or adipocytes (Benoit et al., 2008). The future clinical application of hNPCs for the study and

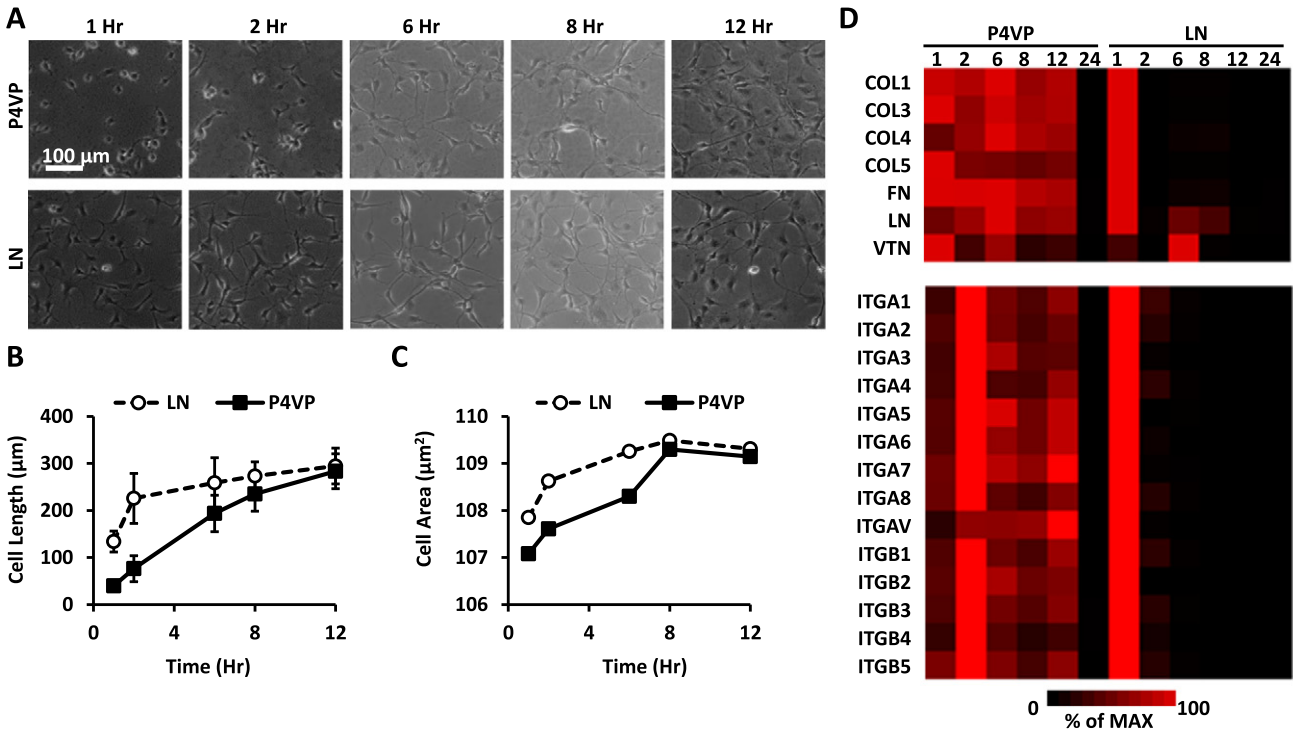

Figure 6 hNPCs cultured on P4VP demonstrate delayed cell attachment and spreading kinetics. (A) Phase contrast images of hNPCs on P4VP and LN at various time points after initial cell seeding. (B) Cell length and (C) cell area were measured on 45 cells from 3 fields at 20× magnification at each time point using Image J (error bars = SD). Populations were compared using Student's *t*-test. $*p < 0.05$, $**p < 0.01$, $***p < 0.001$. Gene expression analysis of (D) endogenous ECMPs and (E) integrins of hNPCs cultured on P4VP and LN at various time points after initial cell seeding. The data is displayed in a heat map where black corresponds to minimum expression levels and red corresponds to maximum levels. For each gene analyzed, the expression levels were normalized to the sample with the highest expression level.

treatment of neurodegenerative disorders will require a similar ability to direct their differentiation into certain fates such as regionally specific neuronal subtypes (Liu and Zhang, 2011). For example, the generation of basal forebrain cholinergic neurons from hNPCs would aid in understanding the mechanisms of Alzheimer's disease (Duan et al., 2014), while hNPC-derived spinal cord motor neurons have the potential to treat spinal cord injuries and motor neuron diseases such as amyotrophic lateral sclerosis (Qu et al., 2014). In the future, unbiased, high-throughput screening approaches, such as the one described in this study, combined with high-throughput surface characterization and regression models (Algahtani et al., 2014), will be useful to engineer synthetic substrates with precise physicochemical properties to precisely direct hNPCs towards these neuronal subtypes.

Several groups have reported the culture and differentiation of fetal or adult neural stem cells (NSCs) on polymer-based substrates (Park et al., 2014; Little et al., 2008; Bhang et al., 2007; Lundin et al., 2011; Saha et al., 2007). It is important to point out that the NSCs used in these studies, which can be isolated from numerous species and various regions in the fetal and adult nervous system, are biologically and developmentally distinct from the hNPCs used in this study (Kornblum, 2007; Temple, 2001). Specifically, the differentiation potential and, thereby, the therapeutic application of NSCs is much more limited than hNPCs, which can differentiate into all the neural lineages (i.e. neurons, astrocytes, and oligodendrocytes) that compromise the central nervous system (CNS) (Chambers et al., 2009; Elkabetz et al., 2008; Shin et al., 2006). Because of these inherent biological differences in NSCs and hNPCs, it is unclear if these substrates that have been previously used for the growth and differentiation of NSCs would have similar efficacy if used with hNPCs. To our knowledge, the synthetic matrix developed in this study is the first demonstration of the use of a defined polymer-based substrate for the culture and differentiation of hNPCs.

In order to have a sufficient number of hNPCs for regenerative medicine and drug screening, efficient methods for their large-scale expansion and differentiation need to be developed. In fact, cell doses for stem cell-based neural therapies have been reported in excess of 6 billion cells per patient (Bretzner et al., 2011; Schwartz et al., 2012; Chen et al., 2013). Although in this study theoretical calculations suggested that 1×10^6 hNPCs cultured on P4VP could be expanded up to 1×10^9 cells in 10 passages (~50 days), practical expansion and differentiation of hNPCs to these numbers are not feasible with current 2D culture systems. Alternatively, microcarriers (MCs), which provide a high-surface area to volume ratio, enable high density cell expansion and scale-up in stirred bioreactors (Reuveny, 1990; Sart et al., 2013). Recently, the use of protein-coated MCs in stirred suspension bioreactors has been reported for the

expansion of several hPSC lines and their derivatives (Sart et al., 2013; Fan et al., 2013; Ting et al., 2014). In the future, the culture of hNPCs on polymer-coated MCs in suspension bioreactors may enable their expansion and differentiation to the numbers required for regenerative medicine purposes.

Conclusions

In this study, we used a high-throughput screening process to identify a synthetic polymer, P4VP, which can support the long-term self-renewal and proliferation of hNPCs at a similar level to cells cultured on purified ECMPs. Moreover, neuronal differentiation of hNPCs was more efficient on P4VP substrates than these traditional ECMP-based substrates. P4VP is chemically defined and available off-the-shelf, thus overcoming the limitations associated with culture on purified ECMPs. Overall, the polymeric biomaterial developed in this study offers a cost-effective, scalable, and robust platform to support the *in vitro* expansion and neuronal differentiation of hNPCs to the quantities needed for disease modeling, drug screening, and cell-based therapies.

Supplementary data to this article can be found online at http://dx.doi.org/10.1016/j.scr.2015.05.002.

Acknowledgments

We thank Mrityunjoy Kar and Shyni Varghese (Department of Bioengineering, University of California-San Diego) for assistance with FTIR-ATR. This research was supported in part by a gift from Michael and Nancy Kaehr, California Institute of Regenerative Medicine (RT2-01889), and funds from the Arizona State University School of Biological and Health Systems Engineering.

References

Algahtani, M.S., Scurr, D.J., Hook, A.L., Anderson, D.G., Langer, R.S., Burley, J.C., et al., 2014. High throughput screening for biomaterials discovery. J. Control. Release 190, 115–126 (Sep 28).

Anderson, D.G., Levenberg, S., Langer, R., 2004. Nanoliter-scale synthesis of arrayed biomaterials and application to human embryonic stem cells. Nat. Biotechnol. 22 (7), 863–866 (Jul).

Bagley, J., Rosenzweig, M., Marks, D.F., Pykett, M.J., 1999. Extended culture of multipotent hematopoietic progenitors without cytokine augmentation in a novel three-dimensional device. Exp. Hematol. 27 (3), 496–504 (Mar).

Banu, N., Rosenzweig, M., Kim, H., Bagley, J., Pykett, M., 2001. Cytokine-augmented culture of haematopoietic progenitor cells in a novel three-dimensional cell growth matrix. Cytokine 13 (6), 349–358 (Mar 21).

Barros, C.S., Franco, S.J., Muller, U., 2010. Extracellular matrix: functions in the nervous system. Cold Spring Harb. Perspect. Biol. 3 (1), a005108 (Jan).

Bellosta, P., Iwahori, A., Plotnikov, A.N., Eliseenkova, A.V., Basilico, C., Mohammadi, M., 2001. Identification of receptor and heparin binding sites in fibroblast growth factor 4 by structure-based mutagenesis. Mol. Cell. Biol. 21 (17), 5946–5957 (Sep).

Benoit, D.S., Schwartz, M.P., Durney, A.R., Anseth, K.S., 2008. Small functional groups for controlled differentiation of hydrogel-encapsulated human mesenchymal stem cells. Nat. Mater. 7 (10), 816–823 (Oct).

Berrios, V.M., Dooner, G.J., Nowakowski, G., Frimberger, A., Valinski, H., Quesenberry, P.J., et al., 2001. The molecular basis for the cytokine-induced defect in homing and engraftment of hematopoietic stem cells. Exp. Hematol. 29 (11), 1326–1335 (Nov).

Betts, K.S., 2010. Growing knowledge: using stem cells to study developmental neurotoxicity. Environ. Health Perspect. 118 (10), A432–A437 (Oct).

Bhang, S.H., Lim, J.S., Choi, C.Y., Kwon, Y.K., Kim, B.S., 2007. The behavior of neural stem cells on biodegradable synthetic polymers. J. Biomater. Sci. Polym. Ed. 18 (2), 223–239.

Bosnjak, Z.J., 2012. Developmental neurotoxicity screening using human embryonic stem cells. Exp. Neurol. 237 (1), 207–210 (Sep).

Bouhon, I.A., Joannides, A., Kato, H., Chandran, S., Allen, N.D., 2006. Embryonic stem cell-derived neural progenitors display temporal restriction to neural patterning. Stem Cells 24 (8), 1908–1913 (Aug).

Brafman, D.A., 2014. Generation, expansion, and differentiation of human pluripotent stem cell (hPSC) derived neural progenitor cells (NPCs). Methods Mol. Biol. 26 (Jul).

Brafman, D.A., de Minicis, S., Seki, E., Shah, K.D., Teng, D., Brenner, D., et al., 2009a. Investigating the role of the extracellular environment in modulating hepatic stellate cell biology with arrayed combinatorial microenvironments. Integr. Biol. (Camb) 1 (8–9), 513–524 (Sep).

Brafman, D.A., Shah, K.D., Fellner, T., Chien, S., Willert, K., 2009b. Defining long-term maintenance conditions of human embryonic stem cells with arrayed cellular microenvironment technology. Stem Cells Dev. 18 (8), 1141–1154 (Oct).

Brafman, D.A., Chang, C.W., Fernandez, A., Willert, K., Varghese, S., Chien, S., 2010. Long-term human pluripotent stem cell self-renewal on synthetic polymer surfaces. Biomaterials 31 (34), 9135–9144 (Dec).

Brafman, D.A., Chien, S., Willert, K., 2012. Arrayed cellular microenvironments for identifying culture and differentiation conditions for stem, primary and rare cell populations. Nat. Protoc. 7 (4), 703–717 (Apr).

Brafman, D.A., Phung, C., Kumar, N., Willert, K., 2013. Regulation of endodermal differentiation of human embryonic stem cells through integrin–ECM interactions. Cell Death Differ. 20 (3), 369–381 (Mar).

Bretzner, F., Gilbert, F., Baylis, F., Brownstone, R.M., 2011. Target populations for first-in-human embryonic stem cell research in spinal cord injury. Cell Stem Cell 8 (5), 468–475 (May 6).

Burgess, W.H., Maciag, T., 1989. The heparin-binding (fibroblast) growth factor family of proteins. Annu. Rev. Biochem. 58, 575–606.

Chambers, S.M., Fasano, C.A., Papapetrou, E.P., Tomishima, M., Sadelain, M., Studer, L., 2009. Highly efficient neural conversion of human ES and iPS cells by dual inhibition of SMAD signaling. Nat. Biotechnol. 27 (3), 275–280 (Mar).

Chen, A.K., Reuveny, S., Oh, S.K., 2013. Application of human mesenchymal and pluripotent stem cell microcarrier cultures in cellular therapy: achievements and future direction. Biotechnol. Adv. 31 (7), 1032–1046 (Nov 15).

Curran, J.M., Chen, R., Hunt, J.A., 2006. The guidance of human mesenchymal stem cell differentiation in vitro by controlled modifications to the cell substrate. Biomaterials 27 (27), 4783–4793 (Sep).

Dalby, M.J., Gadegaard, N., Oreffo, R.O., 2014. Harnessing nanotopography and integrin–matrix interactions to influence stem cell fate. Nat. Mater. 13 (6), 558–569 (Jun).

Duan, L., Bhattacharyya, B.J., Belmadani, A., Pan, L., Miller, R.J., Kessler, J.A., 2014. Stem cell derived basal forebrain cholinergic neurons from Alzheimer's disease patients are more susceptible to cell death. Mol. Neurodegener. 9, 3.

Ehring, B., Biber, K., Upton, T.M., Plosky, D., Pykett, M., Rosenzweig, M., 2003. Expansion of HPCs from cord blood in a novel 3D matrix. Cytotherapy 5 (6), 490–499.

Elkabetz, Y., Panagiotakos, G., Al Shamy, G., Socci, N.D., Tabar, V., Studer, L., 2008. Human ES cell-derived neural rosettes reveal a functionally distinct early neural stem cell stage. Genes Dev. 22 (2), 152–165 (Jan 15).

Fan, H., Hu, Y., Zhang, C., Li, X., Lv, R., Qin, L., et al., 2006. Cartilage regeneration using mesenchymal stem cells and a PLGA-gelatin/chondroitin/hyaluronate hybrid scaffold. Biomaterials 27 (26), 4573–4580 (Sep).

Fan, Y., Hsiung, M., Cheng, C., Tzanakakis, E.S., 2013. Facile engineering of xeno-free microcarriers for the scalable cultivation of human pluripotent stem cells in stirred suspension. Tissue Eng. Part A 7 (Oct).

Gil, J.E., Woo, D.H., Shim, J.H., Kim, S.E., You, H.J., Park, S.H., et al., 2009. Vitronectin promotes oligodendrocyte differentiation during neurogenesis of human embryonic stem cells. FEBS Lett. 583 (3), 561–567 (Feb 4).

Goetz, A.K., Scheffler, B., Chen, H.X., Wang, S., Suslov, O., Xiang, H., et al., 2006. Temporally restricted substrate interactions direct fate and specification of neural precursors derived from embryonic stem cells. Proc. Natl. Acad. Sci. U. S. A. 103 (29), 11063–11068 (Jul 18).

Hansen, A., Mjoseng, H.K., Zhang, R., Kalloudis, M., Koutsos, V., de Sousa, P.A., et al., 2014. High-density polymer microarrays: identifying synthetic polymers that control human embryonic stem cell growth. Adv. Healthcare Mater. 3 (6), 848–853 (Jun).

Hefferan, M.P., Galik, J., Kakinohana, O., Sekerkova, G., Santucci, C., Marsala, S., et al., 2012. Human neural stem cell replacement therapy for amyotrophic lateral sclerosis by spinal transplantation. PLoS One 7 (8) e42614.

Humphries, J.D., Byron, A., Humphries, M.J., 2006. Integrin ligands at a glance. J. Cell Sci. 119 (Pt 19), 3901–3903 (Oct 1).

Imaizumi, Y., Okano, H., 2013. Modeling human neurological disorders with induced pluripotent stem cells. J. Neurochem. 129 (3), 388–399 (May).

Kakinohana, O., Juhasova, J., Juhas, S., Motlik, J., Platoshyn, O., Galik, J., et al., 2012. Survival and differentiation of human embryonic stem cell-derived neural precursors grafted spinally in spinal ischemia-injured rats or in naive immunosuppressed minipigs: a qualitative and quantitative study. Cell Transplant 21 (12), 2603–2619.

Kirby, B.J., Wheeler, A.R., Zare, R.N., Fruetel, J.A., Shepodd, T.J., 2003. Programmable modification of cell adhesion and zeta potential in silica microchips. Lab Chip 3 (1), 5–10 (Feb).

Kornblum, H.I., 2007. Introduction to neural stem cells. Stroke 38 (2 Suppl), 810–816 (Feb).

Kotobuki, N., Katsube, Y., Katou, Y., Tadokoro, M., Hirose, M., Ohgushi, H., 2008. In vivo survival and osteogenic differentiation of allogeneic rat bone marrow mesenchymal stem cells (MSCs). Cell Transplant. 17 (6), 705–712.

Lampin, M., Warocquier, C., Legris, C., Degrange, M., Sigot-Luizard, M.F., 1997. Correlation between substratum roughness and wettability, cell adhesion, and cell migration. J. Biomed. Mater. Res. 36 (1), 99–108 (Jul).

Li, Y., Gautam, A., Yang, J., Qiu, L., Melkoumian, Z., Weber, J., et al., 2012. Differentiation of oligodendrocyte progenitor cells from human embryonic stem cells on vitronectin-derived synthetic peptide acrylate surface. Stem Cells Dev. 22 (10), 1497–1505 (May 15).

Li, Y., Liu, M., Yan, Y., Yang, S.T., 2014. Neural differentiation from pluripotent stem cells: the role of natural and synthetic extracellular matrix. World J. Stem Cells 6 (1), 11–23 (Jan 26).

Li, Y., Liu, M., Yan, Y., Yang, S.T., 2014. Neural differentiation from pluripotent stem cells: The role of natural and synthetic extracellular matrix. World J, Stem Cells 6 (1), 11–23 (Jan 26).

Little, L., Healy, K.E., Schaffer, D., 2008. Engineering biomaterials for synthetic neural stem cell microenvironments. Chem. Rev. 108 (5), 1787–1796 (May).

Liu, H., Zhang, S.C., 2011. Specification of neuronal and glial subtypes from human pluripotent stem cells. Cell. Mol. Life Sci. 68 (24), 3995–4008 (Dec).

Lofti, M., Nejb, M., Naceur, M., 2013. Chapter 8: cell adhesion to biomaterials: concept of biocompatibility in advances in biomaterials science and biomedical applications. Intech 207–240.

Lu, P., Wang, Y., Graham, L., McHale, K., Gao, M., Wu, D., et al., 2012. Long-distance growth and connectivity of neural stem cells after severe spinal cord injury. Cell 150 (6), 1264–1273 (Sep 14).

Lundin, V., Herland, A., Berggren, M., Jager, E.W., Teixeira, A.I., 2011. Control of neural stem cell survival by electroactive polymer substrates. PLoS One 6 (4), e18624.

Ma, W., Tavakoli, T., Derby, E., Serebryakova, Y., Rao, M.S., Mattson, M.P., 2008. Cell–extracellular matrix interactions regulate neural differentiation of human embryonic stem cells. BMC Dev. Biol. 8, 90.

Marchetto, M.C., Winner, B., Gage, F.H., 2010. Pluripotent stem cells in neurodegenerative and neurodevelopmental diseases. Hum. Mol. Genet. 19 (R1), R71–R76 (Apr 15).

Marthiens, V., Kazanis, I., Moss, L., Long, K., Ffrench-Constant, C., 2010. Adhesion molecules in the stem cell niche—more than just staying in shape? J. Cell Sci. 123 (Pt 10), 1613–1622 (May 15).

Mei, Y., Saha, K., Bogatyrev, S.R., Yang, J., Hook, A.L., Kalcioglu, Z.I., et al., 2010. Combinatorial development of biomaterials for clonal growth of human pluripotent stem cells. Nat. Mater. 9 (9), 768–778 (Sep).

Park, M., Shin, M., Kim, E., Lee, S., Park, K.I., Lee, H., et al., 2014. The promotion of human neural stem cells adhesion using bioinspired poly(norepinephrine) nanoscale coating. J. Nanomater. 2014, 1–10.

Pavlov, I., Lauri, S., Taira, T., Rauvala, H., 2004. The role of ECM molecules in activity-dependent synaptic development and plasticity. Birth Defects Res. C Embryo Today 72 (1), 12–24 (Mar).

Qu, Q., Li, D., Louis, K.R., Li, X., Yang, H., Sun, Q., et al., 2014. High-efficiency motor neuron differentiation from human pluripotent stem cells and the function of Islet-1. Nat. Commun. 5, 3449.

Reuveny, S., 1990. Microcarrier culture systems. Bioprocess Technol. 10, 271–341.

Richardson, S.M., Hughes, N., Hunt, J.A., Freemont, A.J., Hoyland, J.A., 2008. Human mesenchymal stem cell differentiation to NP-like cells in chitosan-glycerophosphate hydrogels. Biomaterials 29 (1), 85–93 (Jan).

Saha, K., Irwin, E.F., Kozhukh, J., Schaffer, D.V., Healy, K.E., 2007. Biomimetic interfacial interpenetrating polymer networks control neural stem cell behavior. J. Biomed. Mater. Res. A 81 (1), 240–249 (Apr).

Sart, S., Agathos, S.N., Li, Y., 2013. Engineering stem cell fate with biochemical and biomechanical properties of microcarriers. Biotechnol. Prog. 29 (6), 1354–1366 (Nov–Dec).

Schwartz, S.D., Hubschman, J.P., Heilwell, G., Franco-Cardenas, V., Pan, C.K., Ostrick, R.M., et al., 2012. Embryonic stem cell trials for macular degeneration: a preliminary report. Lancet 379 (9817), 713–720 (Feb 25).

Shin, H., Jo, S., Mikos, A.G., 2003. Biomimetic materials for tissue engineering. Biomaterials 24 (24), 4353–4364 (Nov).

Shin, S., Mitalipova, M., Noggle, S., Tibbitts, D., Venable, A., Rao, R., et al., 2006. Long-term proliferation of human embryonic stem cell-derived neuroepithelial cells using defined adherent culture conditions. Stem Cells 24 (1), 125–138 (Jan).

Smetana Jr., K., Vytasek, R., Stol, M., 1992. Electrostatic interaction influences cell adhesion? Int. J. Hematol. 56 (3), 219–223 (Dec).

Temple, S., 2001. The development of neural stem cells. Nature 414 (6859), 112–117 (Nov 1).

Ting, S., Chen, A., Reuveny, S., Oh, S., 2014. An intermittent rocking platform for integrated expansion and differentiation of human pluripotent stem cells to cardiomyocytes in suspended microcarrier cultures. Stem Cell Res. 13 (2), 202–213 (Sep).

VanGuilder, H.D., Vrana, K.E., Freeman, W.M., 2008. Twenty-five years of quantitative PCR for gene expression analysis. Biotechniques 44 (5), 619–626 (Apr).

Villa-Diaz, L.G., Nandivada, H., Ding, J., Nogueira-de-Souza, N.C., Krebsbach, P.H., O'Shea, K.S., et al., 2010. Synthetic polymer coatings for long-term growth of human embryonic stem cells. Nat. Biotechnol. 28 (6), 581–583 (Jun).

Wade, A., McKinney, A., Phillips, J.J., 2014. Matrix regulators in neural stem cell functions. Biochim. Biophys. Acta 1840 (8), 2520–2525 (Aug).

Warren, L., Manos, P.D., Ahfeldt, T., Loh, Y.H., Li, H., Lau, F., et al., 2010. Highly efficient reprogramming to pluripotency and directed differentiation of human cells with synthetic modified mRNA. Cell Stem Cell 7 (5), 618–630 (Nov 5).

Wilson, M.S., Graham, J.R., Ball, A.J., 2014. Multiparametric high content analysis for assessment of neurotoxicity in differentiated neuronal cell lines and human embryonic stem cell-derived neurons. Neurotoxicology 42, 33–48 (May).

Wojcik-Stanaszek, L., Gregor, A., Zalewska, T., 2011. Regulation of neurogenesis by extracellular matrix and integrins. Acta Neurobiol. Exp. (Wars) 71 (1), 103–112.

Yuan, S.H., Martin, J., Elia, J., Flippin, J., Paramban, R.I., Hefferan, M.P., et al., 2011. Cell-surface marker signatures for the isolation of neural stem cells, glia and neurons derived from human pluripotent stem cells. PLoS One 6 (3), e17540.

Zhang, R., Mjoseng, H.K., Hoeve, M.A., Bauer, N.G., Pells, S., Besseling, R., et al., 2013. A thermoresponsive and chemically defined hydrogel for long-term culture of human embryonic stem cells. Nat. Commun. 4, 1335.

Zhao, F., Grayson, W.L., Ma, T., Bunnell, B., Lu, W.W., 2006. Effects of hydroxyapatite in 3-D chitosan-gelatin polymer network on human mesenchymal stem cell construct development. Biomaterials 27 (9), 1859–1867 (Mar).